Journal of Power Sources 270 (2014) 68–78

Contents lists available at ScienceDirect

Journal of Power Sources

journal homepage: www.elsevier.com/locate/jpowsour

A high precision study of the electrolyte additives vinylene carbonate, vinyl ethylene carbonate and lithium bis(oxalate)borate in $LiCoO_2$/graphite pouch cells

David Yaohui Wang [a], N.N. Sinha [b], J.C. Burns [b], R. Petibon [a], J.R. Dahn [a, b, *]

[a] Department of Chemistry, Dalhousie University, Halifax B3H 4R2, Canada
[b] Department of Physics and Atmospheric Science, Dalhousie University, Halifax B3H 3J5, Canada

HIGHLIGHTS

- VC, VEC and LiBOB additives are studied in $LiCoO_2$/graphite pouch cells.
- High precision coulometry and impedance spectroscopy were used here.
- Additives yielding small parasitic reactions and low resistance films were found.
- VEC and LiBOB used with VC bring benefits in terms of reducing parasitic reactions.

ARTICLE INFO

Article history:
Received 21 January 2014
Received in revised form
8 July 2014
Accepted 9 July 2014
Available online 17 July 2014

Keywords:
Li-ion batteries
Electrolyte additives
Vinylene carbonate
Vinyl ethylene carbonate
Lithium bis(oxalato)borate
Precision coulometry

ABSTRACT

The effects of three well-known electrolyte additives, used singly or in combination, on $LiCoO_2$/graphite pouch cells has been investigated using the ultra high precision charger (UHPC) at Dalhousie University, electrochemical impedance spectroscopy (EIS) and long term cycling Vinylene carbonate (VC), vinyl ethylene carbonate (VEC), and lithium bis(oxalato) borate (LiBOB) were chosen for study. The results show that combinations of electrolyte additives that act synergistically can be more effective than a single electrolyte additive. However, simply using 2% VC yielded cells very competitive in coulombic efficiency (CE), charge endpoint capacity slippage and charge transfer resistance (R_{ct}). For cells with 1% LiBOB and VC (1, 2, 4 or 6%), adding VC above 2% does not increase the CE, but increases the electrode charge transfer impedances. R_{ct} for cells containing 1% LiBOB and VEC (0.5, 1 or 4%) decreased after long term cycling (1800 h), compared to that tested after the UHPC cycling (500 h) indicating that VEC might be useful for the design of power cells. However, the opposite behaviour (increasing R_{ct} with cycle number) was observed for the control cells or cells containing LiBOB and/or VC.

1. Introduction

Extending the lifetime of Li-ion cells to 30–50 years for grid energy applications is one of the most challenging problems remaining for battery researchers. Given that the first Li-ion cells were produced in 1991, there can be no test of Li-ion cells that has lasted for more than 23 years [1]. A limited number of papers [2–4] about long term cycling (for years) of Li-ion cells exist but none of these considers lifetimes of several decades.

The use of electrolyte additives is one of the most effective and economical ways to improve the lifetime of Li-ion cells [5,6]. Vinylene carbonate (VC) [7], for instance, has been regarded as a versatile additive that can yield cells very competitive in a wide variety of properties. Burns et al. [8] studied the impact of VC in wound $LiCoO_2$/graphite and $Li[Ni_{0.42}Mn_{0.42}Co_{0.16}]O_2$/graphite cells with 1 M $LiPF_6$ in ethylene carbonate:ethyl methyl carbonate (EC:EMC, 3:7 vol.% ratio). Burns et al. [8] showed that VC can increase the coulombic efficiency (CE), decrease charge endpoint capacity slippage and decrease self-discharge during storage primarily by slowing down the rate of the electrolyte oxidation at the positive electrode. Zhang et al. [9] demonstrated the beneficial effect of lithium bis(oxalato)borate (LiBOB) as an electrolyte additive in improving the SEI formation at the graphite electrode in $LiBF_4$-PC based electrolyte. Vinyl ethylene carbonate (VEC) was found to be able to prevent the intercalation of the propylene carbonate into graphite by forming a stable passive film [10].

* Corresponding author. Department of Chemistry, Dalhousie University, Halifax B3H 4R2, Canada.
E-mail address: jeff.dahn@dal.ca (J.R. Dahn).

http://dx.doi.org/10.1016/j.jpowsour.2014.07.053
0378-7753/

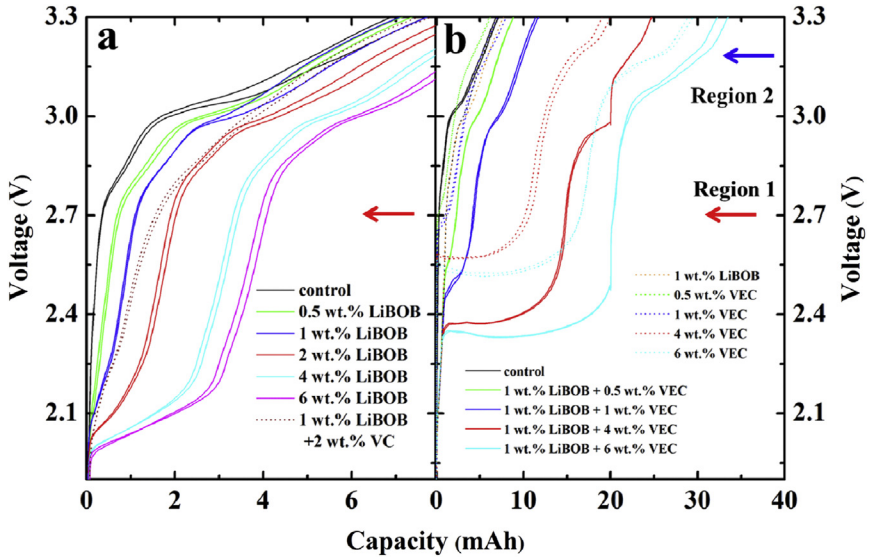

Fig. 1. Voltage versus capacity during (a) the first 8 mAh and (b) the first 40 mAh of the formation cycle at 40 °C of 225 mAh $LiCoO_2$/graphite pouch cells with different electrolyte additives as indicated.

Electrolyte additives are indispensible for the development of improved Li-ion cells.

The synergetic impacts of electrolyte additives on the properties and performance of Li-ion cells are not extensively investigated in literature. Most academic studies have focused on the beneficial effects of a certain electrolyte additive, which is unlikely to be more competitive than a combination of several additives. There is little data available that compares the effectiveness of different additives and additive blends for the same Li-ion cell type. However, limited reports [11–13] showed that a combination of additives that act synergistically can be more effective than a single additive. When different electrode materials and/or electrolytes are used, the impacts of additives can be more complicated.

Our research group uses high precision coulometry [14,15], to detect the parasitic reactions which occur in Li-ion cells to allow us to find electrolyte additives that minimize these reactions. Our previous work [16] illustrated the direct link between increased CE in short term measurements and longer lifetime of cells. Highly reproducible machine-made pouch cells were used in this study in order to ensure that the small differences in CE are caused by the additives and not caused by the differences between the tested cells. High precision CE measurements can therefore help predict the lifetime of Li-ion cells from experiments that take several

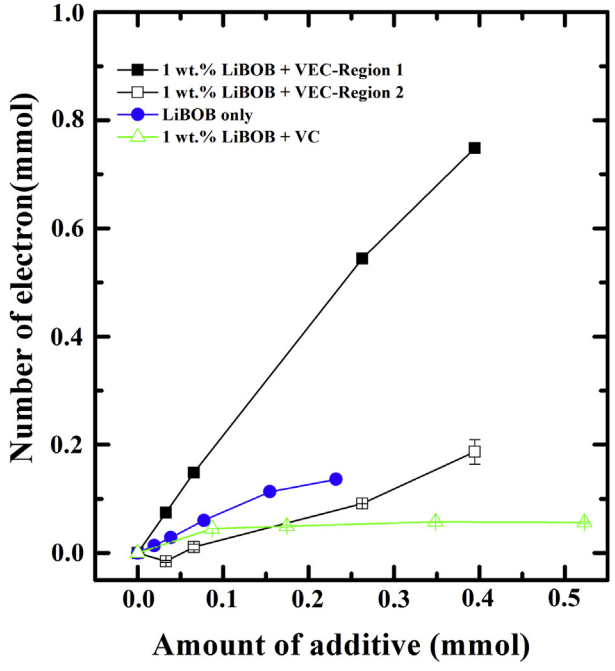

Fig. 2. Number of electrons consumed in the processes occurring in region 1 and region 2 (see Fig. 1) of the formation cycle at 40 °C plotted versus the amount of additive (blue circles: varied LiBOB concentration; black squares: varied VEC concentration) for $LiCoO_2$/graphite pouch cells with different electrolyte additives as indicated. (For interpretation of the references to colour in this figure legend, the reader is referred to the web version of this article.)

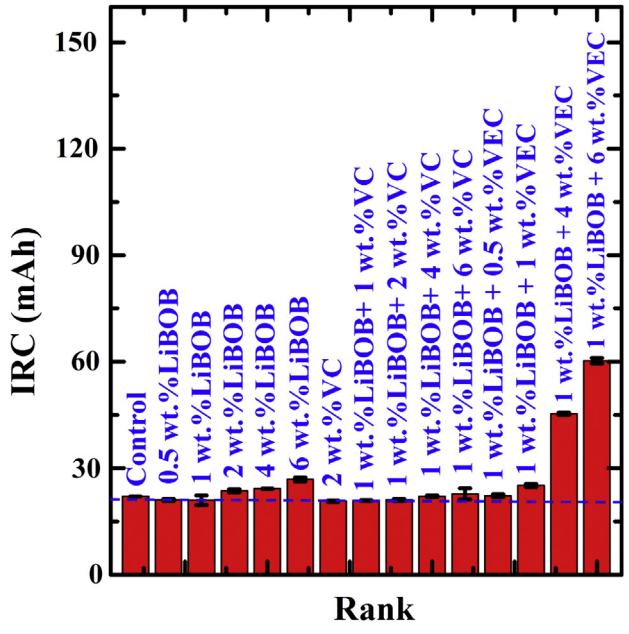

Fig. 3. First cycle irreversible capacity (IRC) for $LiCoO_2$/graphite pouch cells with different electrolyte additives as indicated at 40 °C.

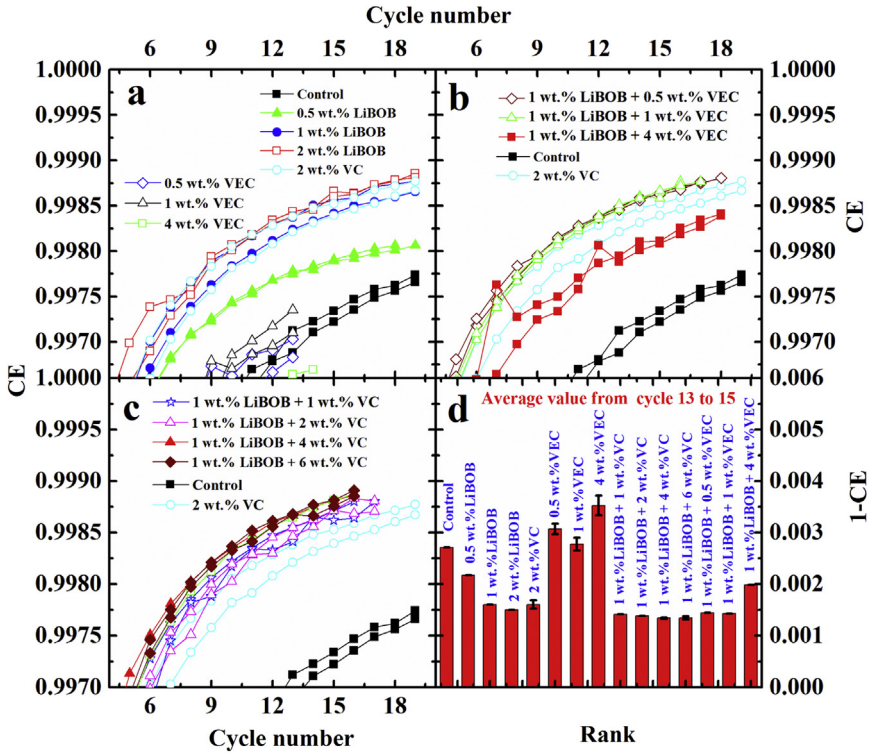

Fig. 4. (a, b and c) CE measured at C/15 and 40°C and (d) a corresponding summary bar chart of the coulombic inefficiency "(1-CE)" for $LiCoO_2$/graphite pouch cells with different electrolyte additives as indicated at 40 °C.

weeks, instead of measuring capacity retention for months or years on a conventional charger. Charge transfer resistance, R_{ct}, at electrode surfaces is another important parameter to be considered to maximize cell lifetime [16]. It is our opinion that simultaneously maximizing CE and minimizing R_{ct} results in the longest lived cells.

Wang et al. recently reported the CE, charge endpoint capacity slippage and R_{ct} of $LiCoO_2$/graphite pouch cells with over 55

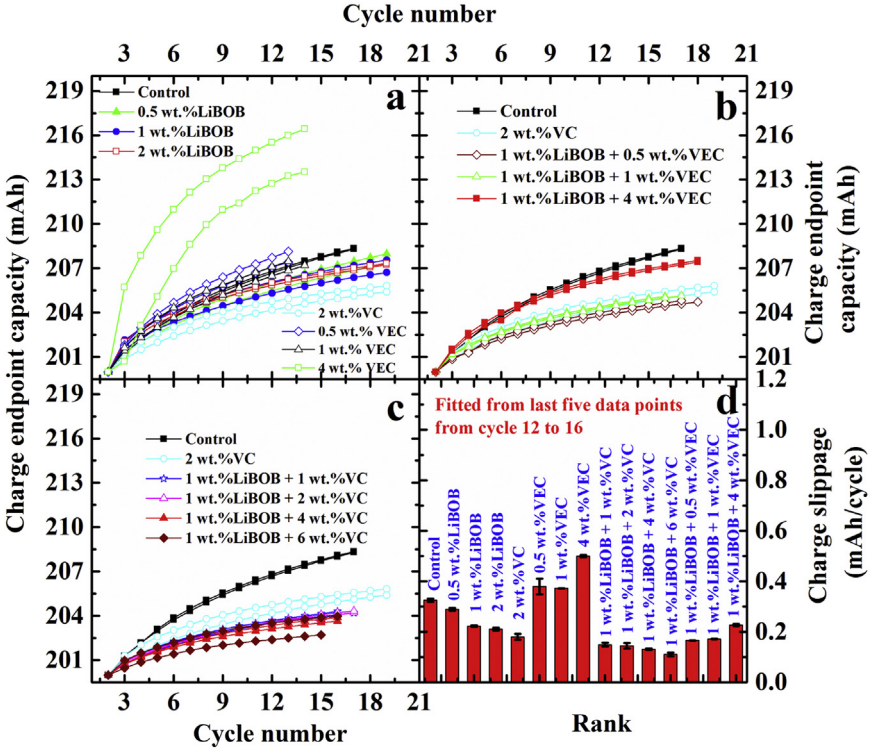

Fig. 5. (a, b and c) Charge endpoint capacity versus cycle number for the same cells as Fig. 4 and (d) a corresponding summary bar chart of the charge endpoint capacity slippage for $LiCoO_2$/graphite pouch cells with different electrolyte additives as indicated at 40 °C.

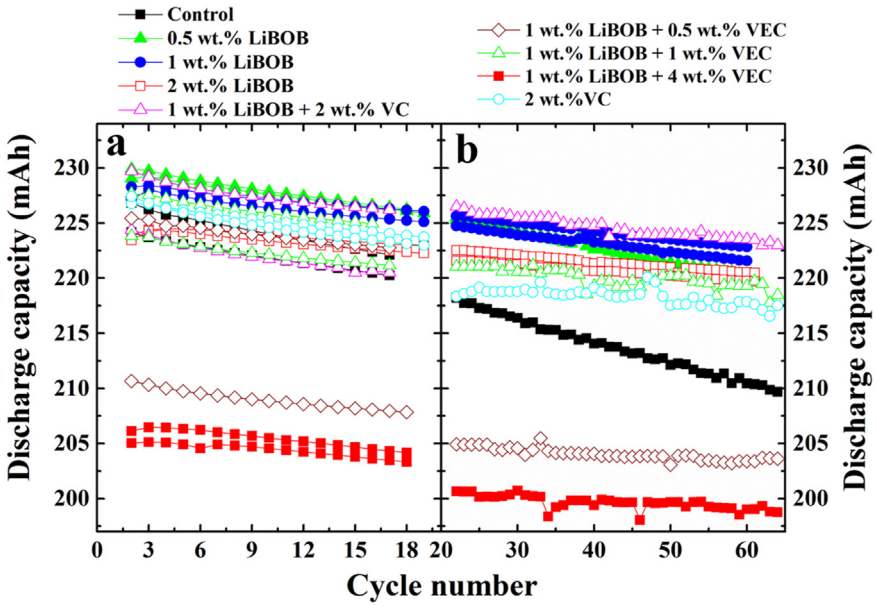

Fig. 6. Discharge capacity versus cycle number for $LiCoO_2$/graphite pouch cells with different electrolyte additives as indicated on (a) UHPC and (b) E-One Moli charger at 40 °C.

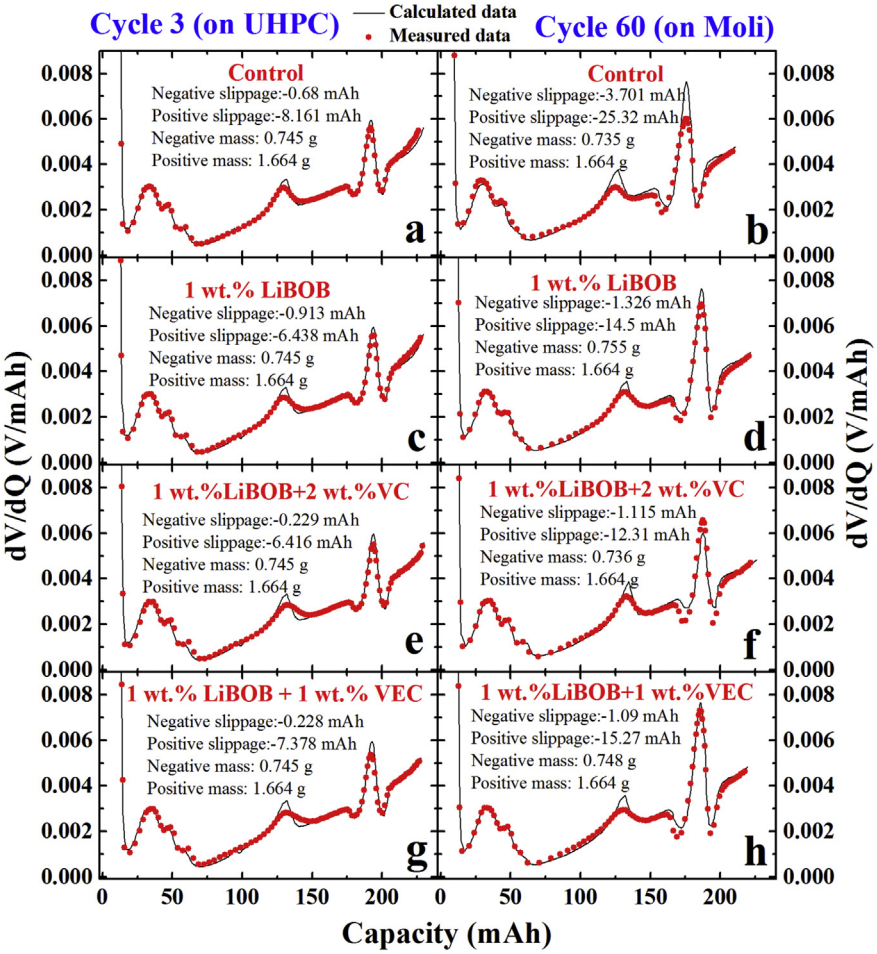

Fig. 7. Calculated and measured d*V*/d*Q* versus capacity for $LiCoO_2$/graphite pouch cells (a and b) without electrolyte additives, (c and d) with 1 wt. % LiBOB, (e and f) 1 wt.% LiBOB + 2 wt.% VC and (g and h) 1 wt.% LiBOB + 1 wt.% VEC, respectively. Cells were tested on the UHPC (a, c, e and g) at cycle 3 and on the E-One Moli cycler (b, d, f and h) at cycle 60. The values of the slippages and active masses are listed as insets. Cells in Fig. 7b, d and h were measured at 30 °C, and the other cells were measured at 40 °C.

different additives or additive combinations in 1 M $LiPF_6$ EC:EMC base electrolyte [17]. That paper gave a review-style presentation of the results and did not go into detail for any electrolyte additive systems. This report focuses on highlighting the work on three well-known electrolyte additives that were studied in Ref. [17] – VC, LiBOB and VEC used as single or multiple additives. The purpose of this more expanded report is to highlight trends and show original data to support and expand upon claims made in Ref. [17].

2. Experimental

Machine-made dry $LiCoO_2$/graphite pouch cells (402030 size, 225 mAh) were supplied by a reputable manufacturer (obtained from Pred Materials Co., 60 East 42nd Street, Suite 1456 New York, NY 10165). All cells were filled with electrolytes and sealed at Dalhousie University. The base electrolyte to which additives were added was 1 M $LiPF_6$ in ethylene carbonate:ethyl methyl carbonate (EC:EMC, 3:7 wt.% ratio, BASF), called the "control" electrolyte here. Vinyl ethylene carbonate (VEC, BASF, >99.9%), vinylene carbonate (VC, BASF, 99.97%) and lithium bis(oxalato) borate (LiBOB, Chemetall, >99.99%), were used as electrolyte additives. In cases where additives yielded promising results, a series of experiments where an additive's concentration was increased stepwise (e.g. 0.5, 1, 2, 4 and 6 wt. %) were performed. Duplicate cells were made for each concentration and additive to ensure repeatability of the measurements.

Several of the dry pouch cells were used to determine the water content in the pouch cell electrodes. A Mettler-Toledo C30 Karl-Fischer analyser equipped with a heated oven was used to evaporate the water from the electrodes into the titrator. The sum of the water contents found in the negative (330 ± 30 ppm) and positive electrodes (640 ± 70 ppm), respectively, would correspond to a level of 1100 ppm water by mass in the electrolyte.

After filling with 0.75 g of electrolyte and vacuum sealing (MTI Corporation, MSK-115A) in an argon-filled glove box, a centrifugal wetting (50 g-force for 20 min) procedure and a 24 h hold at 40.0 ± 0.1 °C and 1.5 V were used to ensure complete wetting of the cell coil. The first charge–discharge cycle (called the formation process here) consisted of charging at 2 mA for the first 10 h then at 15 mA for the rest of the charge to 4.2 V. The cells were then discharged to 3.8 V at 15 mA. Following the formation process, cells were degassed in the glove box and vacuum sealed again.

Cells were cycled using the UHPC between 2.8 and 4.2 V at 40.0 ± 0.1 °C using currents corresponding to C/15 for 15 cycles where comparisons were made. After cycling on the UHPC, electrochemical impedance spectroscopy (EIS, Bio-Logic VMP3), with a 10 mV perturbation and a frequency range from 10 mHz to 100 kHz, was used to measure the combined charge transfer resistance (R_{ct}) of both electrodes in each cell. Before the impedance tests, cells were charged to 3.8 V on a Maccor 4000 series charger and held at 3.8 V until the current dropped below the corresponding C/1000 current, so that all cells were measured under the same conditions. All impedance data were collected at 10.0 and 30.0 ± 0.1 °C. After the first EIS tests, cells were put on a computer controlled charger (produced by E-One Moli Energy Canada Ltd.) for another 50 cycles between 2.8 and 4.2 V at 30.0 ± 0.1 or 40.0 ± 0.1 °C using currents corresponding to C/15. EIS data was measured after these 50 cycles as well. A homemade differential voltage (dV/dQ versus Q) analysis software package [18] was used to investigate the causes of cell capacity loss with cycle number in a few cases.

3. Results and discussion

Fig. 1 shows the voltage as a function of the capacity for cells with different additives during the first 5% (Fig. 1a) or the first 20% (Fig. 1b) of the first charge of these cells (formation cycle). All the cells with additives gave excess capacity below 3.0 V compared to the cells with control electrolyte, presumably due to reduction of additives on the graphite negative electrode. Fig. 1a shows that the excess capacity, primarily in a plateau near 2.1 V, increased as the LiBOB content increased from 0.5% to 6%. Cells containing 1% LiBOB and 2% VC showed more excess capacity than cells containing only 1% LiBOB below 3.0 V (Fig. 1a). With an increased concentration of VC, the voltage versus capacity plots for all the cells with 1% LiBOB and VC (1, 2, 4 or 6%) overlap with each other. Therefore, Fig. 1a only shows data for cells with 1% LiBOB and 2% VC for the sake of clarity. Fig. 1b shows that cells containing 0.5% VEC gave excess capacity around 2.7 V, and the excess capacity increased as VEC content increased to 6%. Furthermore, VEC-containing cells start to show a second plateau near at 3.2 V which also increased in capacity as the VEC content increased. This indicates that two sequential reactions at the graphite negative electrode occur when VEC is present as has been discussed previously [19]. When 1% LiBOB was added into the VEC containing cells, similar behaviour was observed, except that the excess capacity appeared about 0.1 V lower compared to the cells containing VEC only.

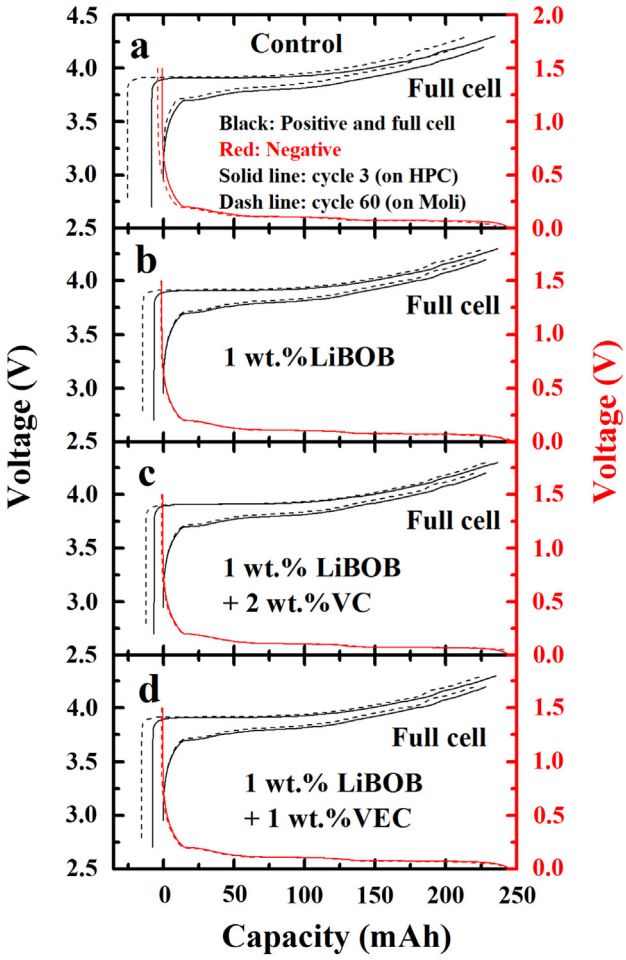

Fig. 8. Full cell (black) as well as positive (black) and negative (red) electrode voltage versus capacity curves derived from the dV/dQ analysis in Fig. 7. The different electrolyte additives are listed in the various panels. The solid lines correspond to cycle 3 and the dashed lines correspond to cycle 60. The relative slippages developed during cycling are easily discerned from this figure. Cells in Fig. 7b, d and h were measured at 30 °C, and the other cells were measured at 40 °C. (For interpretation of the references to colour in this figure legend, the reader is referred to the web version of this article.)

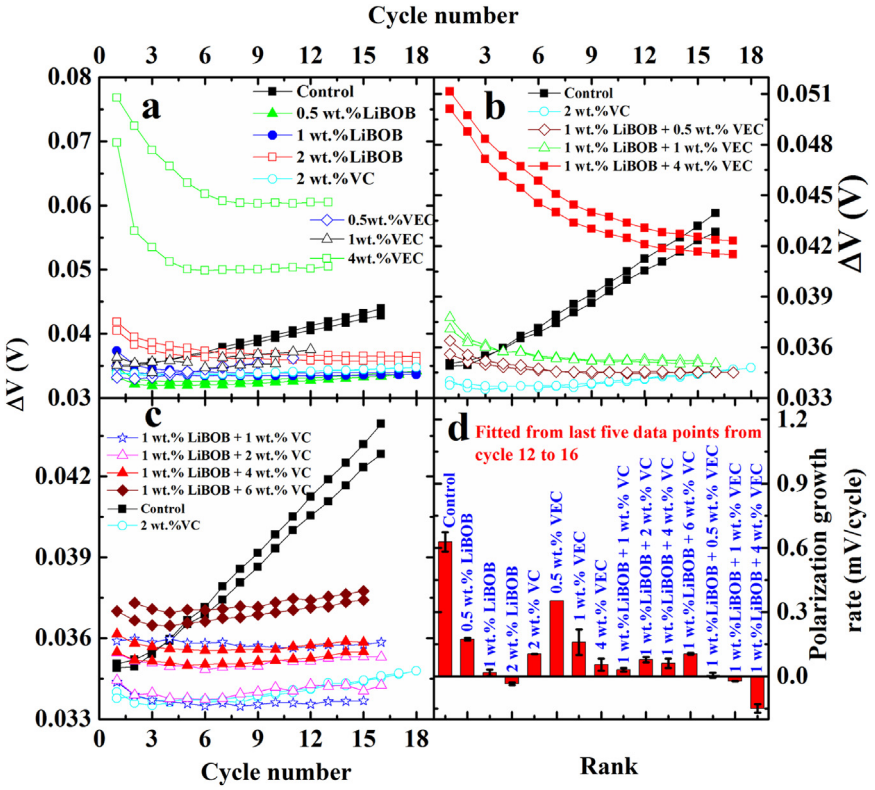

Fig. 9. (a, b and c) Difference between average charge voltage and average discharge voltage (ΔV) as a function of cycle number for $LiCoO_2$/graphite pouch cells cycled at C/15 at 40 °C with and without additives as indicated and (d) summary bar chart of the polarization growth rate for the corresponding cells fitted from cycle 12 to 16. These cells were cycled on the UHPC.

Fig. 2 shows the number of electrons (in mmol) involved in the reduction reactions of the different additives during plateaus at specific voltages (2.1 V (LiBOB), 2.3–2.7 V (first VEC process) and 3.2 V (second VEC process), marked by arrows in Fig. 1) as a function of the amount of additive (in mmol) added to the pouch cell. The number of electrons involved in the "region 1" excess capacity (below 2.7 V) was calculated by subtracting the capacity at 2.7 V for the control cell from the capacity of the additive-containing cell at

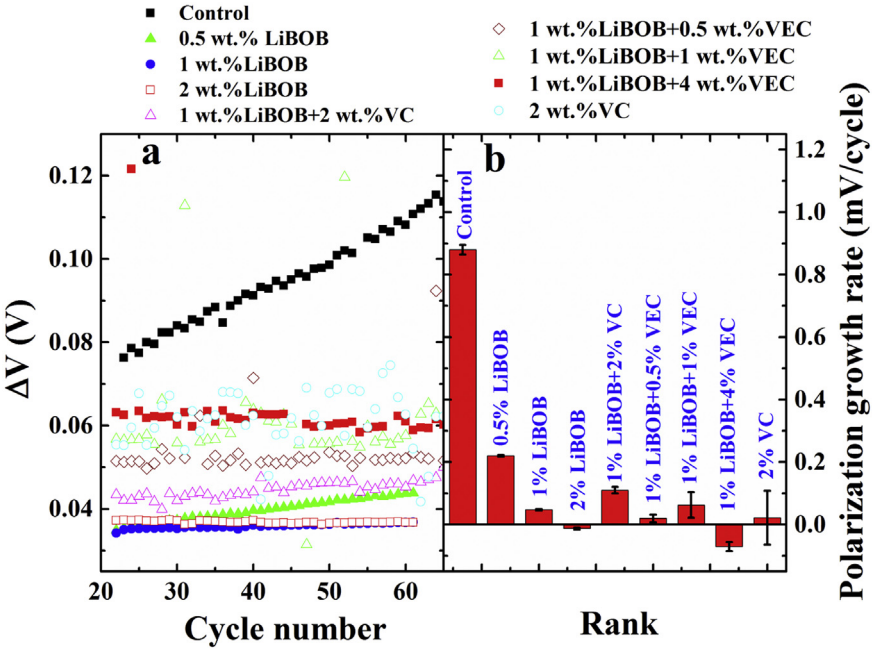

Fig. 10. (a) Difference between average charge voltage and average discharge voltage (ΔV) as a function of cycle number for $LiCoO_2$/graphite pouch cells cycled at C/15 with and without additives as indicated and (b) polarization growth rate for the corresponding cells fitted from cycles 20 to 60. These cells were cycled on the E-One Moli charger after UHPC cycling. Cells with 1 wt.% LiBOB + 2 wt.% VC were measured at 40 °C, and all the other cells were measured at 30 °C.

2.7 V. The number of electrons involved in the "region 2" excess capacity was calculated by subtracting the capacity of the control cell at 3.2 V plus the region 1 capacity from the capacity of the additive-containing cell at 3.2 V. Fig. 2 shows a linear behaviour with a slope of 2 for the region 1 capacity as the amount of VEC is increased in the presence of 1% LiBOB. [The reader should be impressed that all the VEC in the entire cell is being reacted during this initial phase of the formation cycle.] This is consistent with our previous work for cells containing only VEC [19]. When only LiBOB is added, the excess capacity below 2.7 V increases linearly up to 4% LiBOB with a slope near 0.75 electrons per LiBOB molecule. For both VEC and LiBOB, these results suggest that reaction products do not initially passivate the graphite surface well because the excess capacity continually increases with additive content. By contrast, when VC is added to cells containing 1% LiBOB, the number of electrons involved in the excess capacity below 2.7 V increases until 1% VC and then saturates suggesting excellent initial passivation of the graphite electrode. A similar saturation was observed in studies of cells with varying concentrations of VC alone [19].

Figs. 1 and 2 show that cells that contain VEC show a second plateau of excess capacity near 3.2 V and that this capacity increases linearly with VEC content whether LiBOB is present or not. The slope of the region 2 curves in Fig. 2 is about 0.5 electrons per VEC molecule.

Fig. 3 shows the first cycle irreversible capacity loss (IRC) for $LiCoO_2$/graphite pouch cells with different electrolyte additives. The IRC, calculated as the difference between the first charge and discharge capacity, is related to the consumption of Li (Li^+ and electrons) due to reactions with electrolyte (as shown in Fig. 2) which create the SEI on the graphite surface. Furthermore, in pouch cells, the production of gas during the formation cycle can deform the jelly rolls and increase irreversible capacity. Control cells, cells with large amounts of LiBOB and cells with large amounts of VEC were observed to swell appreciably (by up to 2 mL) during formation, before the cells were degassed. The results in Fig. 3 show the same trend as the results in Fig. 2, but the IRC in Fig. 3 is slightly larger than that expected based on Figs. 1 and 2. This difference is thought to be caused by the effects of gassing. One very interesting feature to note is that the IRC of cells with 2% VC is slightly less than that of control cells. This is not expected based on the results in Fig. 2 and also on results from Xiong et al. [20] who showed that irreversible capacity of Li/graphite cells increased with VC content. It is our opinion that this difference can be explained by the reduction in gassing (about 0.2 mL gas for cells with 2% VC compared to 1.0 mL of gas for control cells) brought about by the addition of VC (See Fig. 5 in Ref. [21]) which leads to less jelly roll deformation and better electrode utilization. All pouch cells were degassed and vacuum sealed again after the formation process to ensure that excellent electrode utilization occurred in subsequent tests.

Burns et al. [16] showed that cells with larger coulombic efficiency (CE) usually have a longer lifetime since maximizing CE normally corresponds to minimizing deleterious parasitic reactions in the cell. Fig. 4a–c shows the CE versus cycle number, collected using the UHPC, for $LiCoO_2$/graphite pouch cells with different electrolyte additives. Two cells for each additive combination are shown to demonstrate reproducibility. Cells with additives (except cells with VEC only) show larger CE than the control cells. Fig. 4d shows a summary plot of the coulombic inefficiency (CIE = 1-CE) for the cells described in Fig. 4a–c. The values of (1-CE) were calculated using an average of the values measured during cycles 13–15. Better cells have smaller values of CIE. The error bars in Fig. 4d represent the standard deviation between the results for the pair cells. Fig. 4d shows that cells with VEC alone had higher CIE than the control cells. For cells with LiBOB alone, the CIE decreases as the content of LiBOB is increased from 0.5% to 2%. Cells with 1 or 2% LiBOB exhibited slightly lower CIE than the cells with 2% VC.

Single electrolyte additives are unlikely to be more effective than a combination of additives that act synergistically [16,17]. Fig. 4 shows that cells with 1% LiBOB and VC (1, 2, 4 or 6%) demonstrate lower CIE than cells with VC alone (2%) or LiBOB alone (1 or 2%), indicating a synergetic effect between VC and LiBOB. Moreover, cells with 1% LiBOB and VC (1, 2, 4 or 6%) have a similar CIE indicating that adding more VC does not significantly decrease the CIE in this case. Fig. 4 shows that cells with VEC alone exhibited higher CIE than control cells (Fig. 4a). However, cells with 1% LiBOB and VEC (0.5 or 1%) show lower CIE than the control cells and cells with 1% LiBOB or VEC, indicating a synergetic effect between LiBOB and VEC. Cells with 1% LiBOB and 4% VEC have a larger CIE, but it is still lower than that of the control cells. Data for cells with 1% LiBOB and 6% VEC are not shown here due to the significant bulging in these cells after the UHPC cycling.

Charge endpoint capacity slippage is a measure of parasitic reactions (e.g. electrolyte oxidation) occurring primarily at the positive electrode [22,23]. Because the CE is directly linked to the discharge endpoint capacity slippage according to the conventions we use [24], it is important to consider both the charge endpoint capacity slippage (the slope of the charge endpoint capacity versus cycle number graph) as well as the CE. Fig. 5a–c shows the charge endpoint capacity versus cycle number for $LiCoO_2$/graphite pouch cells with different electrolyte additives. All the charge endpoint capacities were intentionally shifted to the same starting point of 200 mAh at cycle two so that small differences can be easily distinguished. The charge endpoint capacity slippage was calculated from the slope of the charge endpoint capacity versus the cycle number plot from cycles 12 to 16. Fig. 5d shows that cells with additives (except cells with VEC only) exhibit lower charge endpoint capacity slippages than the control cells. Figs. 4d and 5d show similar trends, but there are important differences. Cells with 1% LiBOB and VC (1, 2, 4 or 6%) showed similar CIE, as shown in Fig. 4. However, with increasing VC contents, cells with 1% LiBOB

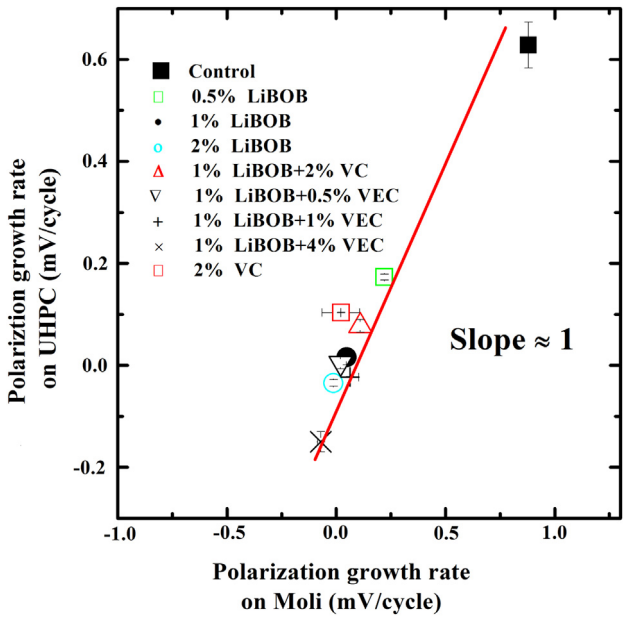

Fig. 11. Polarization growth rate of cells with different additives collected using the UHPC (early cycles – Fig. 9) as a function of the polarization growth rate of cells measured using the E-One Moli charger (cycles 20–60 – Fig. 10). Horizontal error bars (data collected using the E-One Moli charger) are much larger than the vertical error bars (data collected using the UHPC).

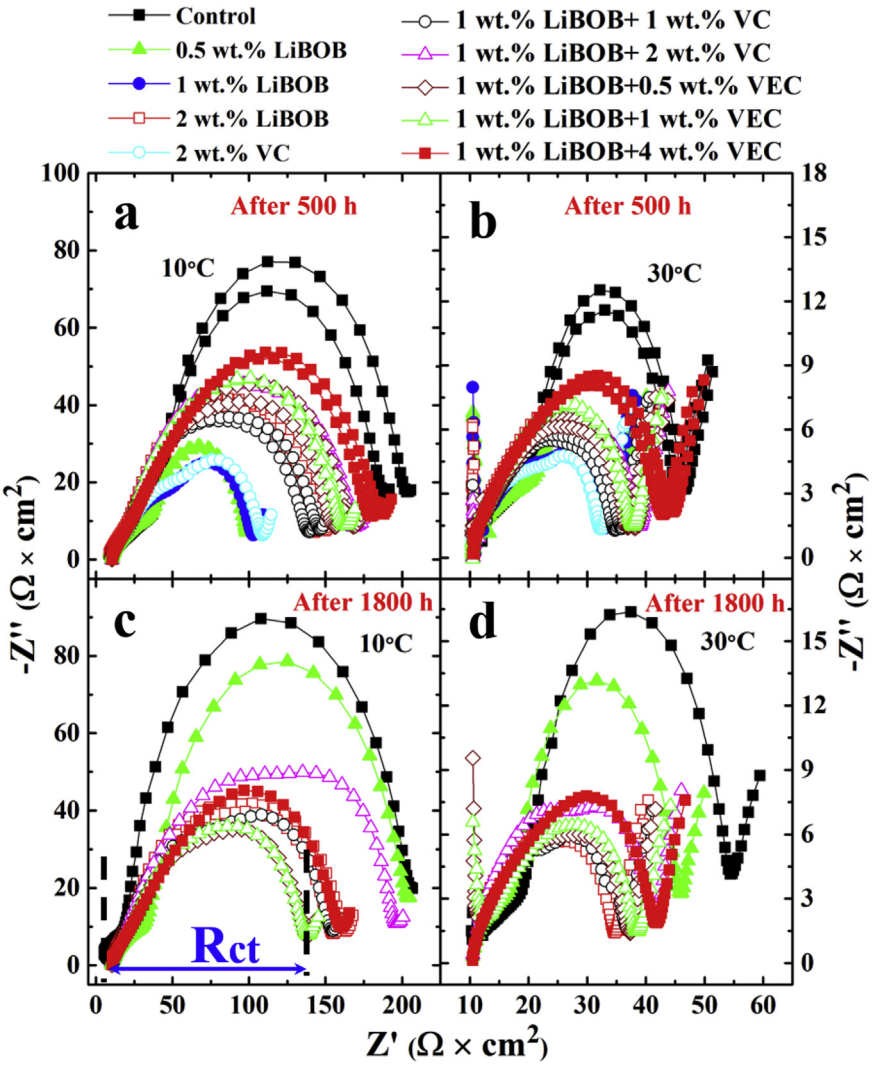

Fig. 12. Nyquist plots for $LiCoO_2$/graphite pouch cells (measured at 3.8 V) with additives as indicated at (a and c) 10 °C and (b and d) 30 °C after (a and b) 500 h of UHPC testing and (c and d) after 1800 h of testing (after the testing on the E-One Moli cycler).

and VC (1, 2, 4 or 6%) show lower and lower charge endpoint capacity slippage, in a manner similar to that found in for VC in previous work [8,19,24]. For cells with 1% LiBOB and VEC (0.5, 1 or 4%), adding more VEC increased the charge endpoint capacity slippage.

Fig. 6 shows the discharge capacity as a function of cycle number for $LiCoO_2$/graphite pouch cells with different electrolytes. The first 20 cycles were performed on the UHPC (Fig. 6a) and the next 50 cycles were carried out on the Moli charger (Fig. 6b). The control cells in Fig. 6b show gradual capacity loss in these relatively short-term low-rate (C/15) experiments, which is due to the loss of active Li ions during solid electrolyte interphase SEI growth [16,25], as will be shown below. Cells with additives generally exhibit better capacity retention than the control cells as anticipated from higher coulombic efficiencies and lower charge endpoint capacity slippage rates. Smith et al. [4] demonstrated that the degradation of $LiCoO_2$/graphite cells tested at low rates is caused by parasitic reactions, which can be detected using the UHPC, instead of by mechanical degradation of the electrodes or by Li-plating at the negative electrode. Previous studies [4,18] showed that dV/dQ analysis can help discern the degradation mechanisms.

Possible causes of cell capacity loss are positive and the negative electrode active material loss, and relative electrode slippage caused by parasitic reactions at each electrode. A homemade dV/dQ analysis software package [18] with four adjustable parameters negative electrode active mass, positive electrode active mass, negative electrode slippage and positive electrode slippage was used in this study. The loss of the positive and the negative electrode active masses is primarily due to the electrical disconnect of electrode particles and should be minimal in well-made $LiCoO_2$/graphite cells tested with modest upper cutoff potentials, like 4.2 V. However, the positive and the negative electrode slippages, ascribed to the oxidation of electrolyte at the positive electrode and the formation of SEI layer at the negative electrode, respectively, are inevitable.

Fig. 7 shows the measured dV/dQ versus capacity curves and illustrative calculated curves for some of the $LiCoO_2$/graphite pouch cells at cycle 3 and cycle 60. The calculated dV/dQ curves were derived from the dV/dQ analysis software using $LiCoO_2$/Li and the graphite/Li coin cell reference data obtained from electrodes taken from an uncycled pouch cell identical to those used to generate the data in Figs. 4–6 [18]. The dV/dQ analysis software adopts the convention suggested by Honkura et al. [26] that the capacity of the fully discharged cell is zero on every cycle. If this is the case, and if the graphite is empty when the Li-ion cell is discharged, then the negative electrode slippage will remain near zero throughout all

cycles. The legend in Fig. 7 shows that this is the case. Fig. 7 shows that the positive electrode slippage is negative and becomes more negative as the cells cycle. This means that the positive electrode is less full of lithium when the graphite is empty in the fully discharged state as cells cycle more and more. Due to the limited resources, the low rate cycle for dV/dQ analysis for cells in Fig. 7b, d and h were measured at 30 °C and the other cells were measured at 40 °C. Fig. 7 shows that cells at cycle 60 exhibit larger relative slippages (negative slippage minus positive slippage) than the corresponding cells at cycle 3, indicating consumption of active lithium in a thickening SEI on the negative electrode. Most important, both the positive and negative active masses are almost constant during the cycling, suggesting that the electrodes in these pouch cells are of good quality. This means the capacity fade observed in Fig. 6 is not caused by problems related to loss of electrode active mass.

The slippage variation in Fig. 7 can be readily examined in Fig. 8, which shows the full Li-ion cell voltage profiles and the correctly scaled reference curves (according to the values in the legend of Fig. 7) for some of the cells with different additives. Due to consumption of Li atoms in the thickening SEI at the graphite negative electrode, the negative electrode voltage–capacity curve slips faster than the positive electrode voltage–capacity curve. Fig. 8 shows that the relative slippage between the positive electrode and negative electrode at cycle 3 and cycle 60 (the distance between the vertical black solid and dashed lines at the left of Fig. 8) for cells with the combination of LiBOB and VC or VEC is smaller than that of the control cells. This shows that the combination of LiBOB and VC or VEC is effective at decreasing the rate of consumption of Li in the SEI at the negative electrode, leading to increased capacity retention. Similar work on the impact of VC is presented in Ref. [18].

Fig. 9a–c shows the difference (ΔV) of the average charge voltage from the average discharge voltage as a function of cycle number for cells with different electrolyte additives (cycled on the UHPC) described by Fig. 4a–c and Fig. 5a–c. The slope of the ΔV–cycle number curve gives an indication of cell impedance variation during cycling, and small slopes of ΔV–cycle number curve are most desirable. The cells with 4% VEC have large values of ΔV because these cells swelled during cycling.

Fig. 9d shows a summary bar chart of the slopes of the ΔV–cycle number curves for the same cells described in Fig. 9a–c. The slope of the ΔV–cycle number curve is called the polarization growth rate in this work, and was fitted from cycle 12 to 16. Cells with additives present lower polarization growth rate than the control cells. For cells with LiBOB alone, the polarization growth rate decreases with increased content of LiBOB (Fig. 9d). Cells with 2% LiBOB show a negative polarization growth rate, which may suggest that the cell impedance decreases over time, and this can be beneficial for the development of long lived cells with lower impedance. Cells with 2% VC show a relatively large polarization growth rate. With increased VC contents, cells with 1% LiBOB and VC (1, 2, 4 or 6%) demonstrate increased polarization growth rate. Cells with 1% LiBOB and 2% VC demonstrate a slightly smaller polarization growth rate than cells with 2% VC, but still larger than cells with 1% LiBOB. Cells with 1% LiBOB and VEC (0.5, 1 or 4%) demonstrate lower polarization growth rate than cells with 1% LiBOB and adding more VEC reduces the polarization growth rate, at the expense of higher initial polarization in the case of cells with 2 and 4% VEC.

Fig. 10 shows ΔV versus the cycle number and the corresponding polarization growth rate for $LiCoO_2$/graphite pouch cells (after the UHPC cycling) with different additives during the longer term cycling on the Moli cycler (cycles shown in Fig. 6b). Noisy data points in Fig. 10a were not excluded and the error in the slopes of the fitted line can be larger than the slopes themselves for some data sets. For the control cells, the polarization growth rate is about 0.84 mV cycle^{-1} during the longer term cycling similar to 0.6 mV cycle^{-1} for data collected on the UHPC. Cells with additives show lower polarization growth rates than the control cells. In order to compare the polarization growth rates between the early and later cycles, Fig. 11 shows the polarization growth rate for data collected on the UHPC plotted as a function of that collected on the Moli charger. The slope of fitted line is near 1, which indicates a good correlation of data collected during short term cycling (20 cycles on the UHPC at currents corresponding to C/15) and longer term cycling (50 subsequent cycles on an E-One Moli charger at currents corresponding to C/15).

Fig. 12 shows Nyquist plots for $LiCoO_2$/graphite pouch cells with different additives at 10 °C or 30 °C, collected after the UHPC cycling (500 h) and after the longer term cycling on the Moli charger

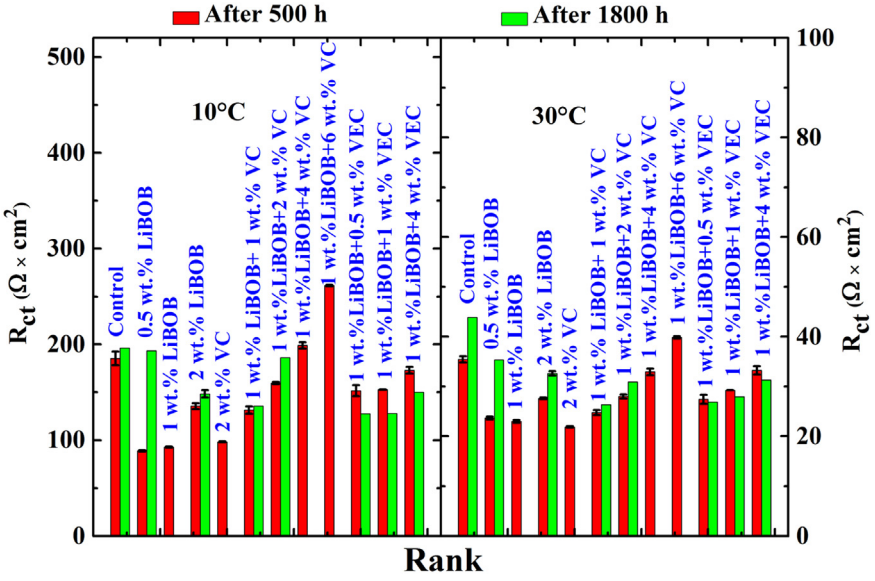

Fig. 13. A summary bar chart for R_{ct} of the same cells shown in Fig. 12 at (a) 10 °C and (b) 30 °C.

(1800 h). The charge transfer resistance (R_{ct}), as marked in Fig. 12c, was taken to be the diameter of the semicircles from the Nyquist plots. The width of the semi-circle is due to the sum of the positive and negative electrode charge transfer resistances. It is important to minimize the width of this semi-circle to create cells with high rate capability. Cells with additives show smaller impedance than the control cells. Cell tested at 10 °C show much larger impedance than cells tested at 30 °C.

Fig. 13 gives a summary of the results in Fig. 12 in order to better compare cell impedance for the cells with the various electrolyte additives. Fig. 13 shows R_{ct} for cells after 500 h (20 cycles) of testing and after 1800 h (70 cycles) of testing both measured at 10 °C and at 30 °C. R_{ct} for cells with LiBOB alone increased with time for each content of LiBOB used in this work. Compared to the cells with 2% LiBOB, R_{ct} of cells containing 0.5% LiBOB increased significantly and was comparable to that of the control cells after 1800 h. It is possible that 0.5% LiBOB is not enough to form effective SEI layers at the positive and negative electrodes, and that the added LiBOB is completely consumed after 1800 h. For cells containing 1% LiBOB and VC (1, 2, 4 or 6%), R_{ct} increased with increased contents of VC in a manner found in cells containing VC only [19,24]. Cells with 1% LiBOB + 6% VC had R_{ct} of 260 Ω × cm^2, similar to R_{ct} of cells with 6% VC (280 Ω × cm^2) measured under the same conditions in a previous study [24]. Interestingly, cells with 1% LiBOB and VEC (0.5, 1 or 4%) demonstrate reduced R_{ct} over time and these cells have small polarization growth rates in Fig. 11. The same trends for R_{ct} at 10 °C (Fig. 13a) were observed at 30 °C in Fig. 13b.

Fig. 14 shows a "radar" plot to summarize the properties of cells with some of the best additive combinations in terms of CIE, charge endpoint capacity slippage, polarization growth rate and R_{ct} at 10 °C. In order to keep the same scale for all four axes, the four properties were scaled as indicated in the figure caption. Different ranges were chosen for the different axes in order to easily distinguish the values. A "better" value is found closer to the origin for each parameter. For example, cells containing LiBOB and VC or VEC show superior performance in CIE, charge slippage and ΔV to cells containing 2% VC alone, but the same cells show larger R_{ct} than cells containing 2% VC alone. Manufacturers can choose different additives or additive combinations for different cell applications. A summary of many more electrolyte additives tested in the same pouch cells can be found in Ref. [17].

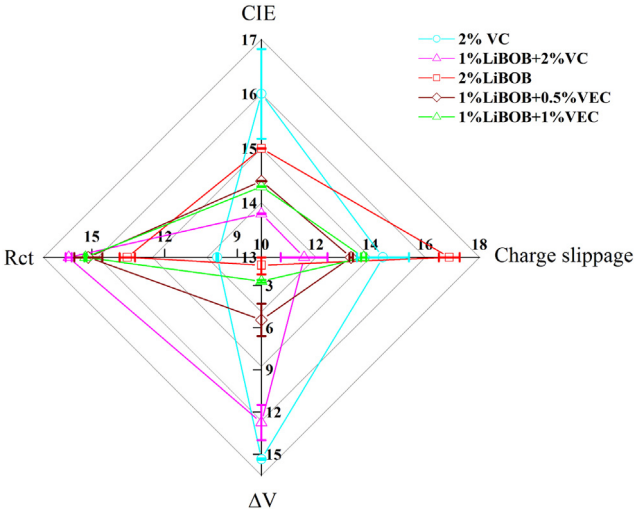

Fig. 14. "Radar" plot to summarize results for cells with additives as indicated. The axes show coulombic inefficiency (CIE = 1-CE, average data between cycle 13–15), charge endpoint capacity slippage (charge slippage, in mAh cycle^{-1}, average data between cycle 12–16), polarization growth rate (in mV cycle^{-1}, average data between cycle 12–16) and charge transfer resistance (R_{ct} measured at 3.8 V and 10 °C after 500 h UPHC cycling, in Ω cm^2). The values in each data set have been scaled (CIE × 10,000, charge slippage × 80, ΔV × 100 + 5, and R_{ct}/10), so they can be compared on the same set of axes.

4. Conclusions

LiBOB, VC and VEC, used either singly or in combination, are useful electrolyte additives for Li-ion cells that can improve CE, reduce charge endpoint capacity slippage and improve cycle life, compared to the control cells. Possible synergies of LiBOB with VC or VEC were investigated in this work. For example, cells containing both LiBOB and VC showed superior performance in CE and charge endpoint capacity slippage to cells containing only 2% VC and cells containing only LiBOB (1 or 2%). Using 2% VC yielded cells very competitive in CE, charge slippage and R_{ct}, so data for the cells containing 2% VC can be used as a baseline to evaluate the effectiveness of different additives for Li-ion cells.

The influences of different electrolyte additives were compared with each other and with the new baseline. Cells with 1% LiBOB and 6% VC were shown to have the lowest CIE and the lowest charge slippage. Unfortunately, the same cells had very high impedance and other experiments (not reported here) show that cells with high VC contents evolve gas during high temperature storage. However, such an electrolyte may be suitable for cells designed only for low rate, long lifetime applications, at moderate temperatures, for example.

Large contents of VC (e.g. 4 or 6%) do not significantly increase the CE, but reduce the charge endpoint capacity slippage and increase the impedance which could be beneficial for long lifetime cells. Cells containing VEC showed reduced impedance over time, but cells with VC and/or LiBOB exhibited increased impedance over time. Cells containing LiBOB and VC or VEC showed superior performance in CIE, charge slippage and ΔV to cells containing 2% VC alone, but the same cells show larger R_{ct} than cells containing 2% VC alone.

Acknowledgements

The authors thank NSERC, 3M Canada for the funding of this work under the auspices of the Industrial Research Chairs program. The authors thank IRM (Institute for Research in Materials at Dalhousie University) and DREAMS (Dalhousie Research in Energy Advanced Materials and Sustainability) for funding. The authors thank Dr. Jing Li and Michael Foran of BASF for providing many of the additives and solvents used in this work.

References

[1] T.B. Reddy, Linden's Handbook of Batteries, fourth ed., The McGraw-Hill Companies Inc., New York, 2010.
[2] M. Broussely, P. Biensan, F. Bonhomme, P. Blanchard, S. Herreyre, K. Nechev, R.J. Staniewicz, J. Power Sources 146 (2005) 90.
[3] G. Jain, in: 30th International Seminar on Primary and Secondary Li Batteries, Ft. Lauderdale, FL, March 11–14, 2013.
[4] A.J. Smith, H.M. Dahn, J.C. Burns, J.R. Dahn, J. Electrochem. Soc. 159 (2012) A705.
[5] S.S. Zhang, J. Power Sources 162 (2006) 1379.
[6] K. Xu, Chem. Rev. 104 (2004) 4303.
[7] B. Simon, J.-P. Boeuve, U.S. Patent No. 5626981, 6 May 1997.
[8] J.C. Burns, N.N. Sinha, D.J. Coyle, G. Jain, C.M. VanElzen, W.M. Lamanna, A. Xiao, E. Scott, J.P. Gardner, J.R. Dahn, J. Electrochem. Soc. 159 (2012) A85.
[9] S.S. Zhang, K. Xu, T.R. Jow, J. Power Sources 156 (2006) 629.
[10] Y. Hu, W. Kong, H. Li, X. Huang, L. Chen, Electrochem. Commun. 6 (2004) 126.
[11] J.C. Burns, N.N. Sinha, G. Jain, H. Ye, C.M. VanElzen, W.M. Lamanna, A. Xiao, E. Scott, J. Choi, J.R. Dahn, J. Electrochem. Soc. 159 (2012) A1095.
[12] J.C. Burns, G. Jain, A.J. Smith, K.W. Eberman, E. Scott, J.P. Gardner, J.R. Dahn, J. Electrochem. Soc. 158 (2011) A255.
[13] J.C. Burns, N.N. Sinha, G. Jain, H. Ye, C.M. VanElzen, W.M. Lamanna, A. Xiao, E. Scott, J. Choi, J.R. Dahn, J. Electrochem. Soc. 159 (2012) A1105.

[14] A.J. Smith, J.C. Burns, S. Trussler, J.R. Dahn, J. Electrochem. Soc. 157 (2010) A196.
[15] T.M. Bond, J.C. Burns, D.A. Stevens, H.M. Dahn, J.R. Dahn, J. Electrochem. Soc. 160 (2013) A521.
[16] J.C. Burns, A. Kassam, N.N. Sinha, L.E. Downie, L. Solnickova, B.M. Way, J.R. Dahn, J. Electrochem. Soc. 160 (2013) A1451.
[17] D.Y. Wang, N.N. Sinha, R. Petibon, J.C. Burns, J.R. Dahn, J. Power Sources 251 (2013) 311.
[18] H.M. Dahn, A.J. Smith, J.C. Burns, D.A. Stevens, J.R. Dahn, J. Electrochem. Soc. 159 (2012) A1405.
[19] R. Petibon, E.C. Henry, J.C. Burns, N.N. Sinha, J.R. Dahn, J. Electrochem. Soc. 161 (2013) A66.
[20] D. Xiong, J.C. Burns, A.J. Smith, N. Sinha, J.R. Dahn, J. Electrochem. Soc. 158 (2011) A1431.
[21] J. Xia, C.P. Aiken, L. Ma, G.Y. Kim, J.C. Burns, L.P. Chen, J.R. Dahn, J. Electrochem. Soc. 161 (2014) A1149–A1157.
[22] J. Christensen, J. Newman, J. Electrochem. Soc. 152 (2005) A818.
[23] A.J. Smith, J.C. Burns, D. Xiong, J.R. Dahn, J. Electrochem. Soc. 158 (2011) A1136.
[24] J.C. Burns, R. Petibon, K.J. Nelson, N.N. Sinha, A. Kassam, B.M. Way, J.R. Dahn, J. Electrochem. Soc. 160 (2013) A1668.
[25] M. Dubarry, C. Truchot, B.Y. Liaw, K. Gering, S. Sazhin, D. Jamison, C. Michelbacher, J. Power Sources 196 (2011) 10336.
[26] K. Honkura, H. Honbo, Y. Koishikawa, T. Horiba, ECS Trans. 13 (2008) 61.